ARTICLE
PUBLISHED ONLINE: 31 OCTOBER 2010 | DOI: 10.1038/NCHEMBIO.467
nature chemical biology

# Inhibitors of protein disulfide isomerase suppress apoptosis induced by misfolded proteins

Benjamin G Hoffstrom[1], Anna Kaplan[1], Reka Letso[1], Ralf S Schmid[2], Gregory J Turmel[2], Donald C Lo[2] & Brent R Stockwell[1,3]*

**A hallmark of many neurodegenerative diseases is accumulation of misfolded proteins within neurons, leading to cellular dysfunction and cell death. Although several mechanisms have been proposed to link protein misfolding to cellular toxicity, the connection remains enigmatic. Here, we report a cell death pathway involving protein disulfide isomerase (PDI), a protein chaperone that catalyzes isomerization, reduction and oxidation of disulfides. Through a small molecule screening approach, we discovered five structurally distinct compounds that prevent apoptosis induced by mutant huntingtin protein. Using modified Huisgen cycloaddition chemistry, we then identified PDI as the molecular target of these small molecules. Expression of polyglutamine-expanded huntingtin exon 1 in PC12 cells caused PDI to accumulate at mitochondrial-associated ER membranes and trigger apoptotic cell death via mitochondrial outer-membrane permeabilization. Inhibiting PDI in rat brain cells suppressed the toxicity of mutant huntingtin exon 1 and Aβ peptides processed from the amyloid precursor protein. This pro-apoptotic function of PDI represents a new mechanism linking protein misfolding and apoptotic cell death.**



Protein folding diseases encompass a large class of neurological disorders, including Alzheimer's disease, Parkinson's disease, amyotrophic lateral sclerosis (ALS), Huntington's disease and prion diseases[1]. Huntington's disease, for example, is a polyglutamine disease caused by a mutation that expands a CAG repeat region within the huntingtin gene. This mutation leads to a polyglutamine-expanded huntingtin protein that improperly folds; ultimately, this causes cell death in the striatum and cortex[2]. Precisely how mutant huntingtin causes Huntington's disease remains unclear; however, markers of apoptotic cell death have been observed in humans and in animal models of Huntington's disease[3–9].

Apoptosis is an elaborate cell death program essential for neuronal pruning during development and for the clearance of cells that become dysfunctional[10]. The most common form of apoptosis proceeds via the intrinsic pathway through mitochondria. In this pathway, an initiation event triggers mitochondrial outer-membrane permeabilization (MOMP), which is a perforation in the outer mitochondrial membrane created by oligomerized Bax or Bak protein[11,12]. The induction of MOMP leads to the release of proteins (for example, cytochrome *c* and Smac) from the mitochondrial intermembrane space, which in turn activates caspase enzymes that degrade key structural and functional components of the cell[13]. Several upstream triggers of MOMP have been reported, including DNA damage, loss of cell adhesion, growth-factor withdrawal and endoplasmic reticulum (ER) stress[14]. The ER is an important site of protein folding, dysregulation of which can activate a cell death cascade. However, in some neurodegenerative diseases (for example, Huntington's and Parkinson's diseases) the aberrant protein accumulates in the cytosol, suggesting additional mechanisms exist to monitor protein folding and to control cellular homeostasis.

We used a cell-based model of Huntington's disease to screen tens of thousands of synthetic compounds and natural products for their ability to suppress cell death induced by polyglutamine-expanded huntingtin exon 1. We then used Huisgen cycloaddition chemistry (or 'click chemistry') to identify PDI as the molecular target of several active compounds. We found that in response to expression of mutant huntingtin exon 1, PDI becomes concentrated at ER-mitochondrial junctions and induces MOMP. The death-suppressing compounds identified in our screen block this cascade by inhibiting the enzymatic activity of PDI. Finally, we show that inhibiting PDI activity in normal rat brain cells suppresses the toxicity of misfolded huntingtin and of Aβ peptides processed from the amyloid precursor protein (APP).

## RESULTS

### Small-molecule inhibitors of apoptosis

To identify small-molecule suppressors of polyglutamine-induced apoptosis, we adapted a PC12 cell model of Huntington's disease into a high-throughput screening format[15]. In this system, PC12 cells were transfected with the first exon of the human huntingtin gene (*HTT*), containing either wild-type (Q25) or mutant (Q103) polyglutamine (polyQ) repeats, fused to enhanced green fluorescent protein (EGFP); we refer to these two cell lines as Q25 and Q103. Protein expression was induced by tebufenozide, an ecdysone analog that binds to the *Bombyx mori* ecdysone receptor. After addition of tebufenozide to the culture medium, mutant cells accumulated peri-nuclear inclusion bodies (~12 h) and underwent apoptosis (15–48 h), which we quantified using Alamar blue, a fluorescent indicator of cell viability (**Fig. 1**).

We screened 68,887 compounds derived from small-molecule libraries containing natural products, natural product analogs, synthetic drug-like compounds and annotated, biologically active compounds (**Fig. 1d**). Hit compounds from the primary screen were prioritized according to their potency in a dose-response curve. These hits were filtered to eliminate those that were probably acting through non–polyQ-dependent mechanisms (for example, compounds that suppress HTT protein expression, or compounds that act as general caspase inhibitors; **Supplementary Fig. 1** and data

[1]Howard Hughes Medical Institute, Department of Biological Sciences, Columbia University, New York, New York, USA. [2]Center for Drug Discovery and Department of Neurobiology, Duke University Medical Center, Durham, North Carolina, USA. [3]Department of Chemistry, Columbia University, New York, New York, USA. *e-mail: bstockwell@columbia.edu

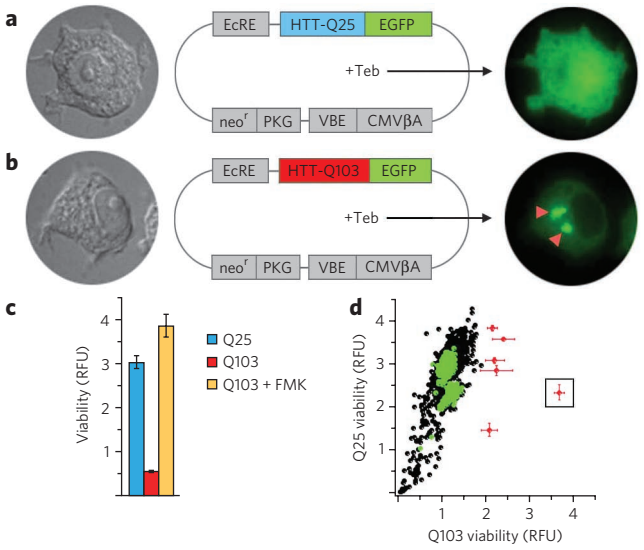


**Figure 1 | Cell-based (PC12) model of mutant huntingtin protein misfolding and cell toxicity.** (**a**) Cells transfected with an inducible plasmid containing wild-type huntingtin exon 1 (HTT-Q25) show diffuse protein expression throughout the cytosol (24 h post-induction with the ecdysone analog tebufenozide, Teb). EcRE, ecdysone responsive element; VBE, VP16-ecdysone receptor chimera; CMV-bA, cytomegalovirus enhancer–β-actin promoter, neor-PKG, neomycin resistance. (**b**) Cells transfected with the same plasmid containing mutant, polyQ-expanded huntingtin exon 1 (HTT-Q103) show perinuclear inclusion bodies at 24 h post-induction (red arrowheads). (**c**) Cell viability of mutant huntingtin–expressing cells is decreased to less than 20% of that of the wild-type huntingtin–expressing cells (measured by Alamar blue fluorescence at 48 h post-induction). Cell death induced by HTT-Q103 can be rescued by treatment with a general caspase inhibitor, Boc-D-FMK (FMK; 50 μM). (**d**) Primary screening results of 2,036 compounds showing effects on cell viability of induced Q25 and Q103 cells. Putative hit compounds that rescue Q103-induced cell death are shown in red; confirmed hit (thiomuscimol **4**) is boxed; DMSO-treated controls are shown in green.

not shown). The top five hits were prioritized according to potency as well as efficacy of cell-viability rescue and the compounds' capacity to restore 'normal' (uninduced) cell morphology to induced Q103-expressing cells (**Fig. 2** and **Supplementary Fig. 2**). Notably, these compounds did not markedly alter the accumulation of HTT-Q103 inclusion bodies (**Supplementary Fig. 3**).

## Identifying small-molecule targets

A covalent interaction between a small molecule and its target protein can increase the facility of target identification. Considering that α-chloromethylketone–like moieties are frequently used for irreversibly inhibiting proteases, we speculated that compound 16F16 (**1**), with its related chloroacetyl moiety, was covalently binding its target protein. In support of this hypothesis, we found that an analog of 16F16 lacking the chloro substituent was inactive. Additional structure-activity studies of 16F16 revealed that changing the ester from methyl to ethyl did not affect its activity. However, modifications at this site that incorporated biotin or fluorescein affinity tags resulted in a complete loss of activity (data not shown). In other words, although we identified a site on 16F16 that could tolerate small structural changes, incorporation of traditional large affinity handles was not compatible with activity (see **Supplementary Methods**).

To overcome this problem, we adapted the copper-mediated Huisgen 1,3,-dipolar cycloaddition of an azide to an alkyne; this reaction has been shown to be bio-orthogonal and facile in the presence of cell lysates[16–20]. The advantage in using this approach was that we could introduce a minimal structural modification to 16F16 (for example, a terminal propargyl alkyne) without losing biological activity. Once the alkyne-derivatized 16F16 was covalently bound to its target protein, we could subsequently attach a tag (for example, fluorescein-azide or rhodamine-azide) via a modified Huisgen cycloaddition reaction (**Fig. 3a**).

After synthesis, we tested the alkyne analog of 16F16 (16F16A (**2**)) for its ability to suppress Q103-induced apoptosis and found that the alkyne modification did not disrupt target binding. We then coupled azidofluorescein to PC12-Q103 lysates treated with 16F16A and purified the resulting fluorescein-tagged proteins with a fluorescein-specific antibody. By MS we identified two isoforms of protein disulfide isomerase (PDIA1 and PDIA3) as specific targets of 16F16A, which we then confirmed by competitive binding assays with labeling of purified PDI and by a western blot of affinity-purified target proteins (**Fig. 3b,c** and **Supplementary Tables 1–3**).

In performing the competitive binding assays, we discovered that in addition to 16F16, the other four active hits from the screen (**Fig. 2**) also showed competitive inhibition of 16F16A binding to PDI,

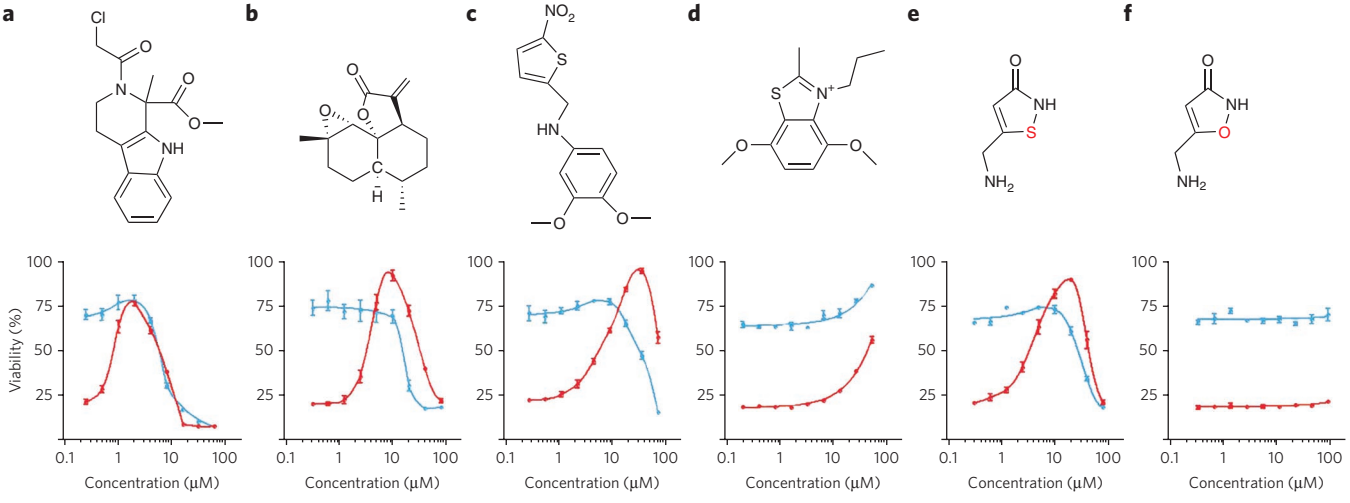


**Figure 2 | Dose-response curves for hit compounds that suppress Q103-induced apoptosis.** The viability of tebufenozide-induced HTT-Q25 (blue) and HTT-Q103 (red) cells was detected by Alamar blue fluorescence and plotted as a percentage of uninduced cells at 48 h post-induction. (**a**) 16F16, (**b**) arteannuin B **5**, (**c**) BBC7M13 (**6**), (**d**) BBC7E8 (**7**), (**e**) thiomuscimol, (**f**) muscimol **8** (inactive analog of thiomuscimol; single-atom substitution shown in red in compound structures).

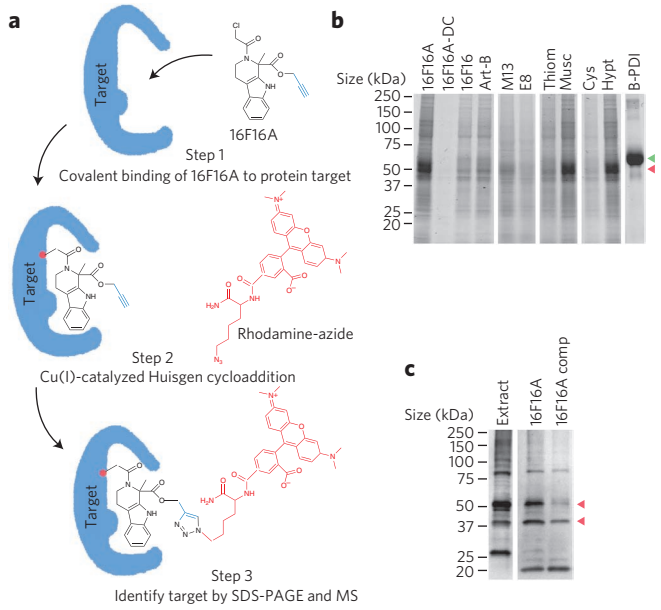


**Figure 3 | Identification of small-molecule target proteins using Huisgen cycloaddition chemistry.** (**a**) Fluorescent tagging of small-molecule target proteins. Step 1, alkyne-derivatized 16F16 (16F16A) covalently binds to target proteins in PC12 lysate. Step 2, 16F16A is coupled to rhodamine-azide via Cu(I)-catalyzed Huisgen 1,3-dipolar cycloaddition reaction. Step 3, fluorescently tagged target proteins are affinity-purified, analyzed by SDS-PAGE and identified by MS as rat PDI precursors (PDIA1 and PDIA3). (**b**) Laser-scanned gel of 16F16A-rhodamine–tagged proteins (PDI appears as a 53-kDa doublet, marked by red arrowhead) in crude PC12 extract. 16F16A-DC **9**, inactive deschloro-16F16 propargyl analog (structure shown in **Fig. 4a**). Pretreatment of PC12 extract with 16F16, arteannuin B (Art-B), BBC7M13 (M13), BBC7E8 (E8), thiomuscimol (Thiom) or cystamine (Cys) blocks 16F16A target binding. Inactive analogs muscimol (Musc) and hypotaurine (Hypt **10**) do not compete for 16F16A target binding. Purified bovine PDI (B-PDI) is covalently labeled by 16F16A-rhodamine (green arrowhead). (**c**) Anti-PDI western blot of affinity-purified 16F16A target proteins confirms the sequence data (full-length 53-kDa and 38-kDa proteolytic PDI fragment; red arrowheads). Extract, crude PC12 extract; 16F16A, affinity-purified 16F16A; the fluorescein-tagged target from PC12 extract; 16F16A comp, pretreatment of PC12 extract with 20× 16F16, followed by addition of 16F16A, fluorescein-azide coupling and affinity purification.

whereas inactive analogs did not (**Fig. 3b**). Given the ability of PDI to function as a disulfide reductase, we tested whether cystamine **3**, a simple organic disulfide that has been shown to delay onset of neuropathological sequellae in animal models of Huntington's and Parkinson's diseases, could compete for 16F16A binding to PDI[21–24]. Cystamine was able to compete with 16F16A for binding to PDI, whereas hypotaurine, an inactive cystamine analog, did not have this effect (**Fig. 3b**). Given the results of the PDI binding experiments, we went on to test these hit compounds, along with cystamine, for their ability to inhibit the enzymatic activity of PDI *in vitro*. We observed a marked correlation between the PDI binding assays (**Fig. 3b**), inhibition of PDI enzymatic activity and rescue of polyQ-induced cell death (**Fig. 4**).

## Mitochondrial-associated membrane PDI induces MOMP

In humans, PDIs (EC 5.3.4.1) constitute a family of at least 17 enzymes of the thioredoxin superfamily that function primarily in the ER as chaperone proteins and facilitate disulfide bond rearrangements via catalysis of thiol-disulfide exchange[25,26]. In addition to their well-described function in the ER, PDI proteins have been reported in the cytosol and on mitochondria, where their physiological functions are less clear[25,27,28]. We examined the localization of PDI over time in subcellular fractions of induced Q25 and Q103 cells and found that after induction, Q103 cells differentially accumulated PDI in the mitochondrial fraction (2.8-fold more than Q25 at 24 h; **Fig. 5a–c**). Inhibiting PDI activity with 16F16 further increased mitochondrial accumulation of PDI in Q103 cells (5.3-fold more than Q25 at 24 h). The latter result suggested that by inhibiting the enzymatic activity of PDI, we were allowing levels of the mitochondrial-associated PDI to increase beyond a point that would otherwise induce apoptosis.

To identify more precisely the location of mitochondrial-associated PDI, we performed protease-shaving analysis of the ER-microsomal and crude (sucrose gradient–purified) mitochondrial fractions. These experiments showed that the mitochondrial-associated PDI was similar to the ER-microsomal PDI in that it was protected from trypsin digestion (**Supplementary Fig. 4**). Mitochondria are known to contact the ER through mitochondrial-associated membranes (MAMs; **Fig. 5d**)[29]. This membrane fraction, which is an extension of the ER that contacts mitochondria, has been shown to function as an important regulatory connection between the ER and mitochondria[30–32]. When we purified MAMs from PC12 mitochondria via Percoll gradient sedimentation, we found that the mitochondrial-associated PDI was predominantly localized to the MAM compartment (**Fig. 5e**).

Inhibiting PDI in Q103-expressing cells suppressed mitochondrial release of cytochrome *c* and subsequent activation of caspases (**Fig. 5f** and **Supplementary Fig. 1**). In light of the finding that increased levels of PDI were associated with mitochondria isolated from Q103-expressing cells, we hypothesized that PDI may engage MOMP by interacting with proapoptotic proteins associated with the outer mitochondrial membrane at a critical concentration ratio. We tested this hypothesis *in vitro* using a 'MOMP assay', in which we added purified PDI to isolated mitochondria and monitored the mitochondrial release of cytochrome *c*. We found that under physiological conditions there was a threshold concentration of PDI that induced MOMP, and that small-molecule PDI inhibitors suppressed this activity (**Fig. 5g**). Finally, overexpressing PDIA1 or PDIA3 in PC12 cells simulated the MOMP assay in a cellular context and induced apoptosis that could be rescued by blocking the catalytic activity of PDI with small-molecule inhibitors (**Fig. 5h,i**).

To further characterize and validate the mechanism of PDI-induced apoptosis, we evaluated the PDI-induced MOMP mechanism in two additional model systems. The induction of MOMP is primarily mediated by the formation of homo-oligomeric channels of Bax or Bak in the mitochondrial outer membrane[12]. Therefore, we tested whether PDI could induce MOMP in mitochondria isolated from wild-type or Bax/Bak double-knockout mouse embryonic fibroblast (MEF) cells[33]. These experiments showed that PDI could induce MOMP in wild-type MEF mitochondria, but mitochondria from Bax/Bak double-knockout cells were resistant (**Fig. 6a**). The mechanism governing the assembly of Bax/Bak homo-oligomeric complexes is not well understood; however, it has been shown that Bax can form an active oligomeric complex via oxidation of conserved cysteine residues[34]. We investigated the possibility that PDI could induce MOMP by oxidizing Bax or Bak and found that wild-type MEF mitochondria undergoing MOMP had disulfide-linked oligomers of Bak, but not Bax (**Fig. 6a** and **Supplementary Fig. 5**). The combined knockdown of Bak and Bax protein in PC12-Q103 cells resulted in an additive rescue of apoptosis, however, suggesting that both Bax and Bak function as downstream cell death effectors (**Supplementary Fig. 6**). Further, overexpressing Bcl-2 protein in PC12-Q103 cells also suppressed apoptosis, suggesting that Bcl-2 can antagonize PDI-induced activation of Bax and Bak (**Supplementary Fig. 6**).

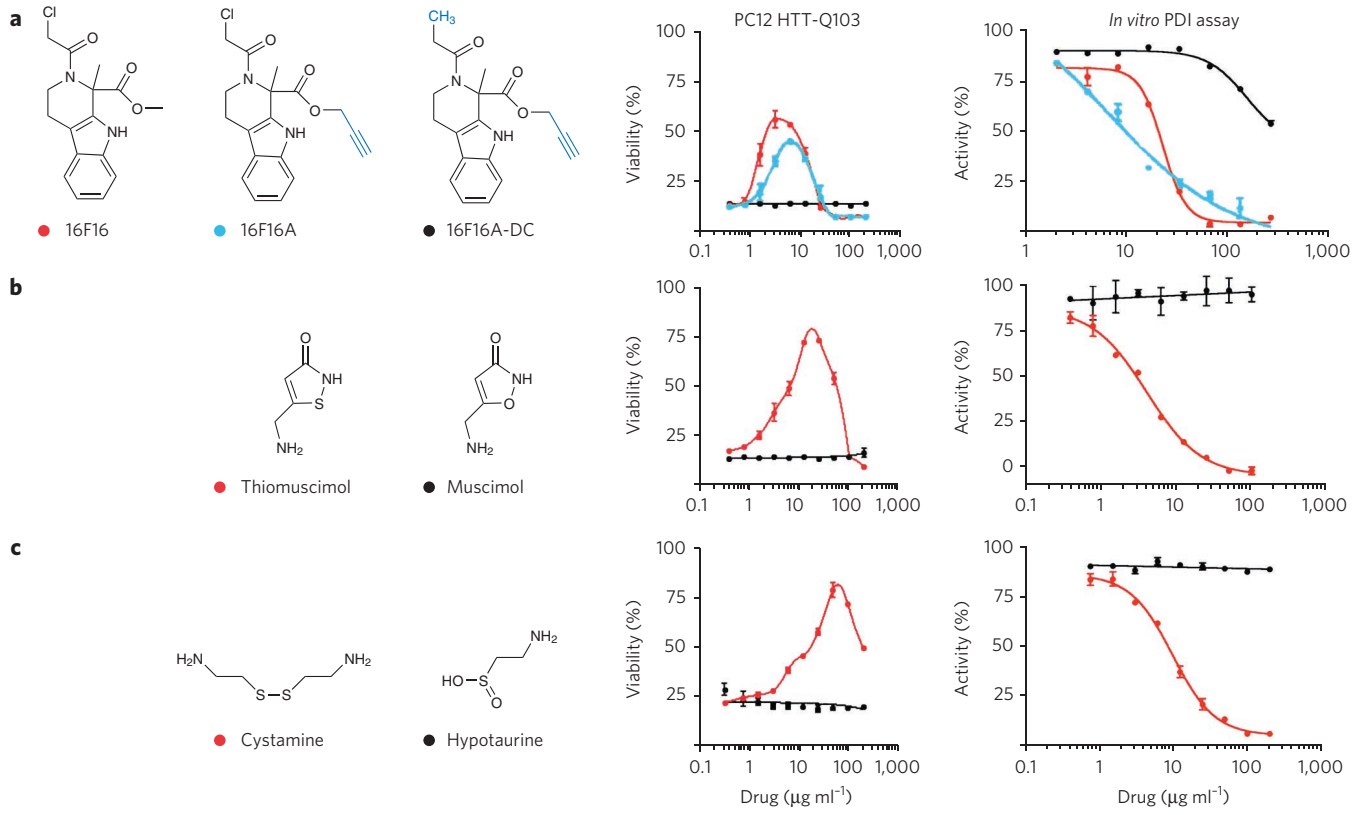


**Figure 4 | Compounds that bind to PDI and rescue HTT-Q103–induced toxicity inhibit PDI reductase activity *in vitro*.** (**a**) 16F16 and 16F16 propargyl analogs (structural modifications shown in blue). (**b**) Thiomuscimol and its inactive analog muscimol. (**c**) Cystamine and its inactive analog hypotaurine.

We next tested the protective effects of PDI inhibitors in a corticostriatal brain-slice model of neurotoxicity induced by mutant HTT exon 1 (HTT-N90Q73)[35–37]. Of three PDI inhibitors tested, all provided dose-dependent rescue of HTT-N90Q73–induced neurotoxicity in medium spiny neurons (MSNs) in the striatal region of the brain slices (**Fig. 6b–e**). We also confirmed the mechanism of PDI-induced toxicity in MSNs by rescuing HTT-N90Q73 neurotoxicity with PDIA3 short hairpin RNA (shRNA; **Fig. 6f** and **Supplementary Fig. 7**).

To broaden the scope of our study, we repeated these experiments in rat brain slices expressing APP, which is processed *in situ* to Aβ peptides, the causative agents central to the amyloid-cascade hypothesis of Alzheimer's disease[38,39]. Similarly to the results for mutant huntingtin, we observed a dose-dependent rescue of Aβ toxicity in pyramidal neurons when PDI was inhibited by small molecules or shRNA knockdown (**Fig. 6g–j**).

## DISCUSSION

Suppressing caspase activation or blocking the release of caspase cleavage products has been shown to be effective in delaying disease progression in transgenic mouse models of ALS, Huntington's disease and Alzheimer's disease[40–45]. In our screen for suppressors of polyQ-induced cell death, we identified several compounds that act upstream of caspase activation by targeting the A1 and A3 isoforms of PDI. As chaperone proteins, PDIs are involved in the recognition and repair of aberrant protein assembly, and their expression is increased in people with ALS, Parkinson's disease and Creutzfeldt-Jakob disease (human prion disease)[46–48]. The initial upregulation of PDIs constitutes a defense mechanism to repair misfolded proteins and restore normal cellular homeostasis[49]. However, as we have shown here in brain-slice assays for neurodegeneration induced by mutant HTT-N90Q73 or by APP/Aβ, small-molecule compounds that limit increases in PDI activity, as well as shRNAs that limit its expression, ultimately provide a net neuroprotective benefit. Thus, analogously to expression of p53, which accumulates to repair damaged DNA but induces apoptosis at extreme levels of DNA damage, PDI is also capable of engaging a cell death cascade when it accumulates at high levels in response to misfolded proteins.

The PDI apoptosis pathway appears to be specific for misfolded proteins, as other apoptotic stimuli (for example, chemical inducers and serum withdrawal) are not suppressed by inhibition of PDI (**Supplementary Fig. 8**). Furthermore, the ability of PDI to induce MOMP in isolated mitochondria and its inhibition-mediated rescue of apoptosis in cells depleted of BiP (also called GRP78), a key regulator of the unfolded protein response, suggests that the PDI pathway operates independently of factors that regulate ER stress–induced apoptosis (**Supplementary Fig. 9**). According to our analysis of PDI-induced MOMP in isolated mitochondria, PDI can oligomerize Bak in the outer mitochondrial membrane by intermolecular oxidation of Bak cysteine residues. Although we have not excluded the involvement of Bak- or Bax-activating intermediates, the structural properties and conserved PDIA1 and PDIA3 residues required for oxidative activity may explain why A1 and A3 were the two PDI isoforms identified in our screen[26].

Complete inhibition of PDI catalytic activity, as observed with high concentrations of inhibitors and knockdown with shRNA, is toxic in cultured cell lines such as PC12. Despite the narrow therapeutic index observed in PC12 cells, our experiments using rat brain-slice explants demonstrate that these treatments protect against polyglutamine and APP/Aβ toxicity in neurons. *In vivo*, cystamine has been shown in several studies to extend survival and improve motor performance in animal models of Huntington's and Parkinson's diseases; however, its mechanism of action has remained unclear[21–24,50]. Here we show that cystamine competitively binds to PDI and inhibits its enzymatic activity *in vitro*. In cells, cystamine suppresses intrinsic apoptosis induced by polyQ-expanded huntingtin and partially blocks PDI-induced MOMP in

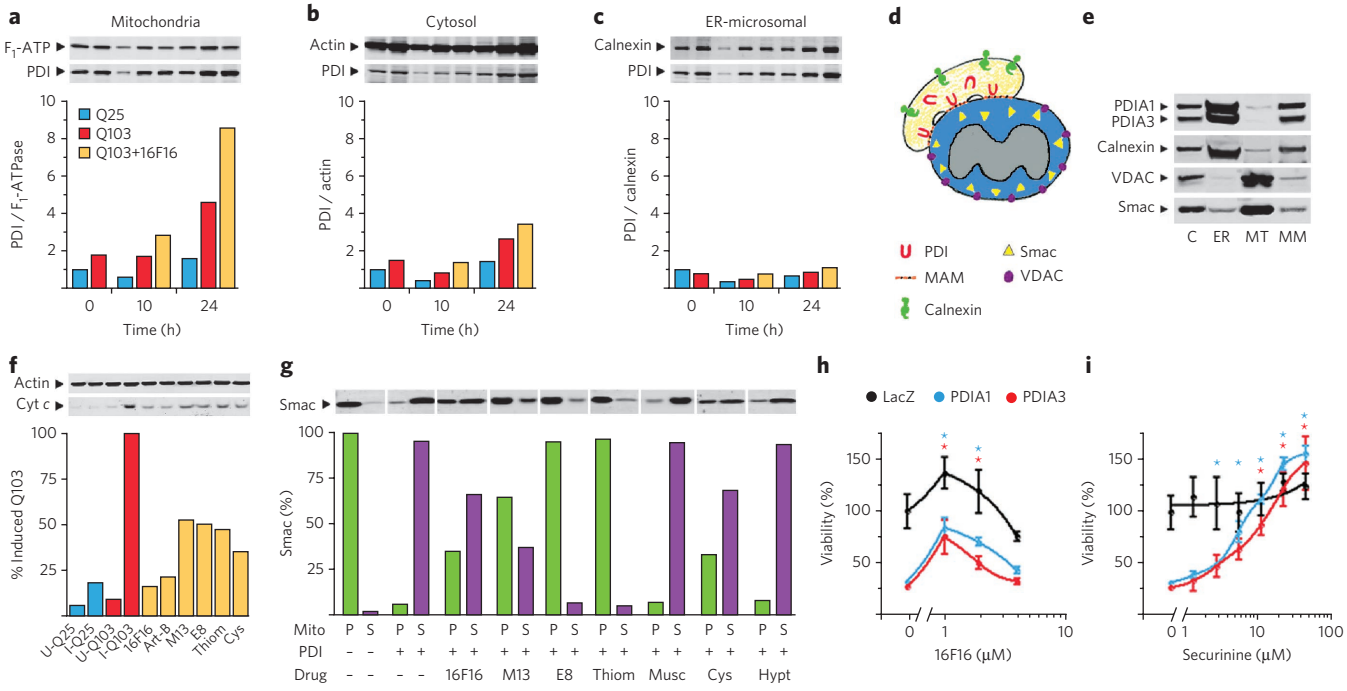


**Figure 5 | PDI accumulates at MAM contacts and induces MOMP.** (**a–c**) Western blot and LI-COR quantification of PDIA1 in mitochondrial, cytosolic and ER-microsomal cell fractions (nomalized to $F_1$-ATPase, actin and calnexin, respectively). Time-course analysis shows a 2.8-fold increase of Q103 mitochondrial PDI over Q25 mitochondrial PDI at 24 h post-induction. Induced Q103 cells rescued with 16F16 (7.8 μM) show a 5.3-fold increase of mitochondrial PDI over induced Q25 cells at 24 h. (**d**) Drawing of the MAM architecture. VDAC is an organelle marker for mitochondria. Smac is a proapoptotic factor localized to the mitochondrial intermembrane space. (**e**) Western blot analysis of purified MAM fractions. Crude (sucrose gradient–purified) mitochondria isolated from Q103-expressing cells were further purified by Percoll gradient centrifugation to isolate the MAM fraction[29]. The MAM fraction is shown to contain PDIA1 and PDIA3 protein. C, crude mitochondria; ER, microsomal-ER fraction; MT, purified mitochondrial fraction; MM, MAM fraction. (**f**) LI-COR quantification of cytosolic cytochrome *c* in Q25- and Q103-expressing cells. U, induced; I, induced; PDI inhibitors are denoted as in **Figure 3**. (**g**) Mitochondrial MOMP assay using purified PC12 mitochondria. The mitochondria were pelleted and MOMP was quantified as a percentage of Smac released from the mitochondrial pellet (P) into the supernatant (S). PDI inhibitors suppress PDI-driven MOMP, whereas inactive analogs muscimol (Musc) and hypotaurine (Hypt) do not suppress Smac release. (**h,i**) Overexpressing PDIA1 or PDIA3 in PC12 cells induces apoptosis that is suppressed by PDI inhibitors ($P < 0.01$ for rescue compared with untreated cells, calculated by ANOVA and Dunnett's *post hoc* comparison test). **Supplementary Figure 10** shows the characterization of securinine **11**, which we identified as an additional PDI inhibitor.



purified mitochondria. These results suggest that the protective effect of cystamine in Huntington's-disease and Parkinson's-disease model mice may occur through inhibition of PDI.

In summary, we used a novel strategy to identify PDI as a target of several compounds that suppress polyglutamine-induced and APP/Aβ-induced neuronal degeneration. Furthermore, we have identified a cell death pathway regulated by PDI, a chaperone protein important for quality control in protein folding. A comprehensive understanding of how the PDI cell death pathway is controlled may aid the discovery of therapeutics to treat protein-misfolding diseases.

## METHODS

**Cell culture and transfection.** We used a PC12 model of Huntington's disease for screening[15]. Briefly, PC12 cells transfected with pBWN, an ecdysone-responsive expression vector containing DNA inserts encoding exon 1 of human huntingtin (including a proline-rich segment and either 25 or 103 mixed CAG and CAA repeats, EGFP and a neomycin-resistance gene) were propagated (37 °C, 9.5% $CO_2$) in complete medium: DMEM high-glucose, 25 mM HEPES (Mediatech no. 15-018-CV), 10% (vol/vol) Cosmic calf serum (HyClone no. SH30087.03), penicillin and streptomycin, 2 mM glutamine and 500 μg $ml^{-1}$ active geneticin (G418). For transgene expression, tebufenozide (gift from Lynne Moore, Gage laboratory, Salk Institute) was added to the above medium (200 nM final concentration from 1 mM stock in 85% ethanol). Wild-type and Bax/Bak double-knockout MEF cells (provided by Craig B. Thompson, University of Pennsylvania) were grown in RPMI medium with penicillin and streptomycin and 10% (vol/vol) fetal bovine serum (Gibco no. 26140-079).

**Cycloaddition reactions and in-gel fluorescence scanning.** Cell lysates were prepared from 24-h-induced Q103 cells by swelling ($23 \times 10^6$ cells $ml^{-1}$ in sodium phosphate buffer, pH 8.1, 5 min, 4 °C), passing through a 30-gauge needle (ten strokes), and clarified (14,000*g*, 20 min, 4 °C). Clarified crude cell lysate (43 μl, $2 \times 10^6$ cell equivalents) was incubated with alkyne-derivatized probe (16F16A or 16F16A-DC, 7 μmol, 1 h, room temperature), and Cu(I)-catalyzed Huisgen cycloaddition reactions (using $RhN_3$ or $FcN_3$ tags) were carried out as described[20]. Labeled lysates were prepared for SDS-PAGE analysis and visualized in-gel using Molecular Dynamics Fluorimager 595 and appropriate excitation and emission filters for the fluorophore. Competitive binding assays were performed as described above, except that cell lysates were preincubated for 1 h at room temperature with 20× molar excess of the tested compound (competition controls were incubated with inactive analogs or equivalent addition of DMSO or water). Cystamine (C121509), hypotaurine (H1384) and bovine PDI (P3818) were purchased from Sigma-Aldrich.

**Affinity purification and MS sequence identification.** Uncoupled $FcN_3$ tag was removed from 16F16A-fluorescein–labeled lysates using Zebra desalting columns (Pierce no. 89882). Labeled proteins were affinity-purified over anti-fluorescein–coupled affinity matrix (5 mg monoclonal anti-fluorescein coupled to NHS-activated sepharose, Amersham no. 17-0906-01) and eluted with 100 mM glycine (pH 2.8). Affinity-purified proteins were analyzed by SDS-PAGE, and fluorescently tagged targets (major doublet at 53–57 kDa) were excised from the gel and submitted to Taplin Biological Mass Spectrometry Facility (Harvard Medical School) for protein identification. Tandem samples were run on SDS-PAGE and transferred to PVDF membranes for western blot analysis using PDI antibody.

**Brain-slice assays for Huntington's disease and Alzheimer's disease.** Coronal brain slices (250 μm thick) containing both cortex and striatum were prepared from CD Sprague-Dawley rat pups (Charles River) at postnatal day 10 using a Vibratome device. Brain slices were placed in six-well plate transwell inserts (BD Biosciences), under which culture medium was added, containing 15% (vol/vol) heat-inactivated horse serum, 10 mM KCl, 10 mM HEPES, 100 U $ml^{-1}$ penicillin-streptomycin, 1 mM sodium pyruvate and 1 mM L-glutamine in Neurobasal A (Invitrogen).

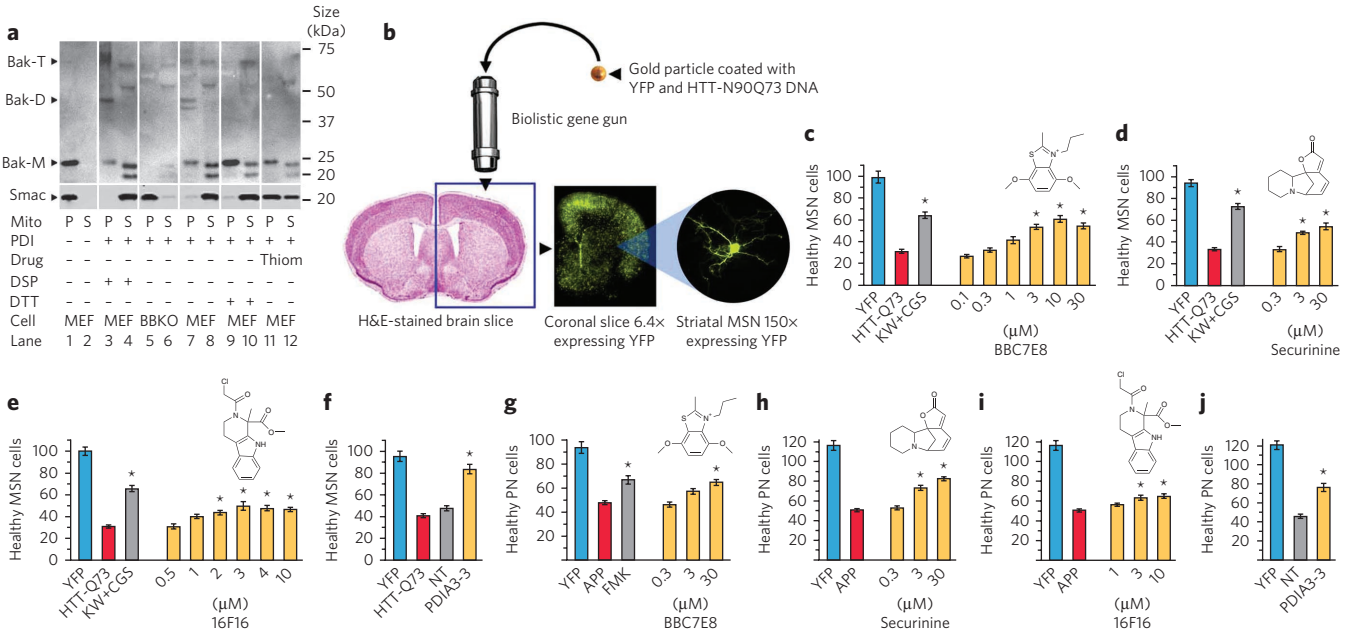


**Figure 6 | Characterization of PDI-induced MOMP and validation in model systems.** (**a**) Mitochondrial MOMP assay using wild-type MEF and Bax/Bak double-knockout (BBKO) MEF cells. Western blot analysis for Smac and Bak protein shows that PDI-induced MOMP takes place in the absence of cytosol and is mediated by oligomerization of mitochondrial Bak (lanes 1–6; Bak-M, Bak-D and Bak-T denote Bak monomer, dimer and trimer, respectively). The Bak protein is oligomerized via oxidation of cysteine residues (lanes 7–10). Oligomerization of Bak and mitochondrial release of Smac is suppressed by inhibition of PDI with thiomuscimol (Thiom; lanes 11 and 12). DSP, dithiobis (succinimidyl) propionate, a homobifunctional and membrane-permeable cross-linker. (**b**) Schematic diagram of the rat corticostriatal brain-slice assay (data in **c**–**j**). (**c**–**e**) The small-molecule PDI inhibitors BBC7E8 (**c**), securinine (**d**) and 16F16 (**e**) suppress HTT-N90Q73–induced toxicity in brain-slice MSNs. (**f**) Knockdown of PDIA3 using a validated A3-3 shRNA targeting plasmid (**Supplementary Fig. 7**) suppresses HTT-N90Q73 toxicity in brain-slice MSNs. (**g**–**i**) APP/Aβ toxicity in brain-slice pyramidal neurons is suppressed by the PDI inhibitors BBC7E8 (**g**), securinine (**h**) and 16F16 (**i**), and by PDIA3 shRNA (**j**). Controls and legend: YFP, transfection control; KW+CGS, chemical rescue of HTT-N90Q73 by KW-6002 and CGS21680; NT, nontargeting shRNA; FMK, caspase inhibitor Boc-D-FMK, 100 μM; PN, pyramidal neurons; yellow bars, inhibitor-treated (PDI inhibitor or shRNA) HTT-N90Q73– or APP/Aβ-expressing cells; $^*P < 0.05$ (by ANOVA followed by Dunnett's *post hoc* comparison test) for rescue of HTT-N90Q73 or APP/Aβ toxicity.

A biolistic device (Helios Gene Gun; Bio-Rad) was then used to transfect brain slices according to manufacturer's instructions; 1.6 μm gold particles were used with the device set at 95–105 pounds per square inch (p.s.i.) and an aperture distance of ~2.5 cm. As the cotransfection linkage rate of biolistics approaches 100%, multiple DNAs can be reliably coexpressed in neurons by coating the gold particles with mixtures of independent expression plasmids[39]. Thus, labeling of striatal or cortical neurons was done by mixing a separate plasmid driving yellow fluorescent protein (YFP) expression together with either an HTT or APP expression construct, as described below, and a third plasmid expressing shRNA was added to the mixture for the RNA-interference knockdown studies. In all cases, total DNA load was balanced in control conditions where necessary by the addition of the corresponding empty vectors. Compounds were added to the culture wells at the time of slice preparation and transfection, to a final DMSO concentration of 0.1% (vol/vol); the slices were then placed in humidified incubators under 5% $CO_2$ at 32 °C.

For the Huntington's-disease brain-slice model, YFP-cotransfected MSNs were identified after 4 d of incubation by their location within the striatum and by their characteristic dendritic arborization using Leica MZFLIII fluorescent stereomicroscopes. MSNs were scored as 'healthy' if they showed normal-sized cell bodies, even and continuous expression of YFP within all cell compartments, and more than two discernable primary dendrites that were more than two cell bodies long. The HTT plasmid used to induce neurodegeneration of MSNs included human HTT exon 1 containing a 73-polyglutamine repeat and was constructed from clones and sequences that were gifts from Chris Ross (Johns Hopkins University) and the Hereditary Disease Foundation. This HTT sequence was cloned into the gWiz expression vector (Genlantis). The positive control was KW+CGS (KW-6002 (50 μM) and CGS-21680 (30 μM)) or the general caspase inhibitor Boc-D-FMK (Sigma-Aldrich, 100 μM).

For the Alzheimer's-disease brain-slice model, cortical pyramidal neurons were assayed after 3 d of incubation and were readily discerned and unambiguously identified by their characteristic positioning and orientation within the cortex, and by their striking morphological features, most notably the extension of a single, prominent apical dendrite radially toward the pial surface. Several key features were used to determine the numbers of healthy cortical pyramidal neurons, namely (i) a robust and brightly labeled cell body positioned within the pyramidal neuronal layers of the cortex; (ii) the retention of a clear apical dendrite extending radially toward the pial surface of the slice; (iii) the extension directly from the cell soma of more than two clear basal dendrites more than two cell body diameters long; and (iv) clear and continuous cytoplasmic labeling with the YFP visual marker in the cell soma as well in all dendrites and the axon. In this brain-slice assay, transfection of the normal human neural APP sequence (695-residue form) produces sufficient Aβ to induce neurodegeneration of cortical neurons, and this neurodegeneration can be blocked by either β- or γ-secretase inhibitors[39]. As above, this APP sequence was cloned into the gWiz expression vector.

**Statistics.** Primary screening parameters were adjusted (for example, cell density and incubation time) to yield the best $Z'$ calculation between induced Q103 and Boc-D-FMK–rescued cells. Mean and s.d. for viability assays (run as biological triplicates) were plotted using Cricket Graph (interpolation function). For the *in vitro* PDI assay and drug/serum-withdrawal apoptosis assay, nonlinear regression was used to fit curves to the mean and s.d. ($n = 3$) calculated with GraphPad Prism software. For western blot quantification, one representative sample of three or more experiments is shown. Statistical significance of shRNA rescue in PC12 cells was determined by ANOVA and Dunnett's *post hoc* comparison test at the 0.01 confidence level. For the corticostriatal brain-slice assay, statistical significance was determined by ANOVA followed by Dunnett's *post hoc* comparison test at the 0.05 confidence level.

Received 10 August 2010; accepted 8 October 2010; published online 31 October 2010

## References

1. Gregersen, N. Protein misfolding disorders: pathogenesis and intervention. *J. Inherit. Metab. Dis.* **29**, 456–470 (2006).
2. Orr, H.T. & Zoghbi, H.Y. Trinucleotide repeat disorders. *Annu. Rev. Neurosci.* **30**, 575–621 (2007).
3. Hickey, M.A. & Chesselet, M.F. Apoptosis in Huntington's disease. *Prog. Neuropsychopharmacol. Biol. Psychiatry* **27**, 255–265 (2003).

4. Thomas, L.B. *et al.* DNA end labeling (TUNEL) in Huntington's disease and other neuropathological conditions. *Exp. Neurol.* **133**, 265–272 (1995).
5. Reddy, P.H. *et al.* Behavioural abnormalities and selective neuronal loss in HD transgenic mice expressing mutated full-length HD cDNA. *Nat. Genet.* **20**, 198–202 (1998).
6. Hodgson, J.G. *et al.* A YAC mouse model for Huntington's disease with full-length mutant huntingtin, cytoplasmic toxicity, and selective striatal neurodegeneration. *Neuron* **23**, 181–192 (1999).
7. Kiechle, T. *et al.* Cytochrome C and caspase-9 expression in Huntington's disease. *Neuromolecular Med.* **1**, 183–195 (2002).
8. Yu, Z.X. *et al.* Mutant huntingtin causes context-dependent neurodegeneration in mice with Huntington's disease. *J. Neurosci.* **23**, 2193–2202 (2003).
9. Ciammola, A. *et al.* Increased apoptosis, Huntingtin inclusions and altered differentiation in muscle cell cultures from Huntington's disease subjects. *Cell Death Differ.* **13**, 2068–2078 (2006).
10. Bredesen, D.E., Rao, R.V. & Mehlen, P. Cell death in the nervous system. *Nature* **443**, 796–802 (2006).
11. Chipuk, J.E. & Green, D.R. How do BCL-2 proteins induce mitochondrial outer membrane permeabilization? *Trends Cell Biol.* **18**, 157–164 (2008).
12. Leber, B., Lin, J. & Andrews, D.W. Embedded together: the life and death consequences of interaction of the Bcl-2 family with membranes. *Apoptosis* **12**, 897–911 (2007).
13. Jiang, X. & Wang, X. Cytochrome C-mediated apoptosis. *Annu. Rev. Biochem.* **73**, 87–106 (2004).
14. Chipuk, J.E., Bouchier-Hayes, L. & Green, D.R. Mitochondrial outer membrane permeabilization during apoptosis: the innocent bystander scenario. *Cell Death Differ.* **13**, 1396–1402 (2006).
15. Aiken, C.T., Tobin, A.J. & Schweitzer, E.S. A cell-based screen for drugs to treat Huntington's disease. *Neurobiol. Dis.* **16**, 546–555 (2004).
16. Huisgen, R. in *1,3-Dipolar Cycloaddition Chemistry* (ed. Padwa, A.) 1–176 (Wiley, New York, 1984).
17. Rostovtsev, V.V., Green, L.G., Fokin, V.V. & Sharpless, K.B. A stepwise huisgen cycloaddition process: copper(I)-catalyzed regioselective "ligation" of azides and terminal alkynes. *Angew. Chem. Int. Edn Engl.* **41**, 2596–2599 (2002).
18. Tornøe, C.W., Christensen, C. & Meldal, M. Peptidotriazoles on solid phase: [1,2,3]-triazoles by regiospecific copper(i)-catalyzed 1,3-dipolar cycloadditions of terminal alkynes to azides. *J. Org. Chem.* **67**, 3057–3064 (2002).
19. Wang, Q. *et al.* Bioconjugation by copper(I)-catalyzed azide-alkyne [3 + 2] cycloaddition. *J. Am. Chem. Soc.* **125**, 3192–3193 (2003).
20. Speers, A.E. & Cravatt, B.F. Profiling enzyme activities in vivo using click chemistry methods. *Chem. Biol.* **11**, 535–546 (2004).
21. Karpuj, M.V. *et al.* Prolonged survival and decreased abnormal movements in transgenic model of Huntington disease, with administration of the transglutaminase inhibitor cystamine. *Nat. Med.* **8**, 143–149 (2002).
22. Dedeoglu, A. *et al.* Therapeutic effects of cystamine in a murine model of Huntington's disease. *J. Neurosci.* **22**, 8942–8950 (2002).
23. Van Raamsdonk, J.M. *et al.* Cystamine treatment is neuroprotective in the YAC128 mouse model of Huntington disease. *J. Neurochem.* **95**, 210–220 (2005).
24. Tremblay, M.E. *et al.* Neuroprotective effects of cystamine in aged parkinsonian mice. *Neurobiol. Aging* **27**, 862–870 (2006).
25. Wilkinson, B. & Gilbert, H.F. Protein disulfide isomerase. *Biochim. Biophys. Acta* **1699**, 35–44 (2004).
26. Ellgaard, L. & Ruddock, L.W. The human protein disulphide isomerase family: substrate interactions and functional properties. *EMBO Rep.* **6**, 28–32 (2005).
27. Rigobello, M.P., Donella-Deana, A., Cesaro, L. & Bindoli, A. Distribution of protein disulphide isomerase in rat liver mitochondria. *Biochem. J.* **356**, 567–570 (2001).
28. Turano, C., Coppari, S., Altieri, F. & Ferraro, A. Proteins of the PDI family: unpredicted non-ER locations and functions. *J. Cell. Physiol.* **193**, 154–163 (2002).
29. Vance, J.E. Phospholipid synthesis in a membrane fraction associated with mitochondria. *J. Biol. Chem.* **265**, 7248–7256 (1990).
30. Rizzuto, R. *et al.* Close contacts with the endoplasmic reticulum as determinants of mitochondrial $Ca^{2+}$ responses. *Science* **280**, 1763–1766 (1998).
31. Hayashi, T. & Su, T.P. Sigma-1 receptor chaperones at the ER-mitochondrion interface regulate $Ca^{2+}$ signaling and cell survival. *Cell* **131**, 596–610 (2007).
32. Hayashi, T., Rizzuto, R., Hajnoczky, G. & Su, T.P. MAM: more than just a housekeeper. *Trends Cell Biol.* **19**, 81–88 (2009).
33. Lindsten, T. *et al.* The combined functions of proapoptotic Bcl-2 family members bak and bax are essential for normal development of multiple tissues. *Mol. Cell* **6**, 1389–1399 (2000).
34. Nie, C. *et al.* Cysteine 62 of Bax is critical for its conformational activation and its proapoptotic activity in response to H2O2-induced apoptosis. *J. Biol. Chem.* **283**, 15359–15369 (2008).
35. Khoshnan, A. *et al.* Activation of the IκB kinase complex and nuclear factor-κB contributes to mutant huntingtin neurotoxicity. *J. Neurosci.* **24**, 7999–8008 (2004).
36. Varma, H., Cheng, R., Voisine, C., Hart, A.C. & Stockwell, B.R. Inhibitors of metabolism rescue cell death in Huntington's disease models. *Proc. Natl. Acad. Sci. USA* **104**, 14525–14530 (2007).
37. Southwell, A.L. *et al.* Intrabodies binding the proline-rich domains of mutant huntingtin increase its turnover and reduce neurotoxicity. *J. Neurosci.* **28**, 9013–9020 (2008).
38. Thinakaran, G. & Koo, E.H. Amyloid precursor protein trafficking, processing, and function. *J. Biol. Chem.* **283**, 29615–29619 (2008).
39. Braithwaite, S.P. *et al.* Inhibition of c-Jun kinase provides neuroprotection in a model of Alzheimer's disease. *Neurobiol. Dis.* **39**, 311–317 (2010).
40. Friedlander, R.M., Brown, R.H., Gagliardini, V., Wang, J. & Yuan, J. Inhibition of ICE slows ALS in mice. *Nature* **388**, 31 (1997).
41. Ona, V.O. *et al.* Inhibition of caspase-1 slows disease progression in a mouse model of Huntington's disease. *Nature* **399**, 263–267 (1999).
42. Chen, M. *et al.* Minocycline inhibits caspase-1 and caspase-3 expression and delays mortality in a transgenic mouse model of Huntington disease. *Nat. Med.* **6**, 797–801 (2000).
43. Zhu, S. *et al.* Minocycline inhibits cytochrome c release and delays progression of amyotrophic lateral sclerosis in mice. *Nature* **417**, 74–78 (2002).
44. Graham, R.K. *et al.* Cleavage at the caspase-6 site is required for neuronal dysfunction and degeneration due to mutant huntingtin. *Cell* **125**, 1179–1191 (2006).
45. Galvan, V. *et al.* Reversal of Alzheimer's-like pathology and behavior in human APP transgenic mice by mutation of Asp664. *Proc. Natl. Acad. Sci. USA* **103**, 7130–7135 (2006).
46. Atkin, J.D. *et al.* Induction of the unfolded protein response in familial amyotrophic lateral sclerosis and association of protein-disulfide isomerase with superoxide dismutase 1. *J. Biol. Chem.* **281**, 30152–30165 (2006).
47. Conn, K.J. *et al.* Identification of the protein disulfide isomerase family member PDIp in experimental Parkinson's disease and Lewy body pathology. *Brain Res.* **1022**, 164–172 (2004).
48. Yoo, B.C. *et al.* Overexpressed protein disulfide isomerase in brains of patients with sporadic Creutzfeldt-Jakob disease. *Neurosci. Lett.* **334**, 196–200 (2002).
49. Uehara, T. *et al.* S-nitrosylated protein-disulphide isomerase links protein misfolding to neurodegeneration. *Nature* **441**, 513–517 (2006).
50. Bailey, C.D. & Johnson, G.V. The protective effects of cystamine in the R6/2 Huntington's disease mouse involve mechanisms other than the inhibition of tissue transglutaminase. *Neurobiol. Aging* **27**, 871–879 (2006).


## Acknowledgments

We thank E. Schweitzer (University of California–Los Angeles) for the transfected PC12 cell lines; C. Ross (Johns Hopkins University) for HTT DNAs upon which the constructs used here were based; I. Smukste for assistance with organic synthesis; A. Bauer for compound library assembly library; D. Dunn for additional brain-slice experiments; C. Thompson (University of Pennsylvania) for the Bax/Bak double-knockout MEF cells; L. Moore (Gage laboratory, Salk Institute) for tebufenozide; A. Speers, J. Alexander and B. Cravatt for reagents and advice on the cycloaddition reactions; E. Miller, E. Signer, A. Tobin, N. Wexler, C. Johnson, R. Pacifici and M. Finn for useful discussions; and E. Miller and S. Hoffschmidt for editorial comments on the manuscript. This research was supported by grants from the US National Institutes of Health (NIGMS 1RO1GM085081 to B.R.S. and NINDS R21NS048181 to D.C.L.), the Hereditary Disease Foundation (D.C.L., B.R.S.), the High Q Foundation (B.R.S.), CHDI Foundation (D.C.L., B.R.S.), the Arnold and Mabel Beckman Foundation (B.R.S.), the Training Program in Molecular Biophysics (T32GM008281 to A.K.) and a Burroughs Wellcome Fund Career Award at the Scientific Interface (B.R.S.). B.G.H. was supported in part by a postdoctoral fellowship from the High Q Foundation. B.R.S. is an Early Career Scientist of the Howard Hughes Medical Institute.

## Author contributions

B.G.H. and B.R.S designed the experiments. B.G.H. performed the experiments and analyzed the data with B.R.S. A.K. assisted with the library screening, characterization of hit compounds, analysis of synthesized analogs, validation studies and structural identification of securinine. R.L. performed the PDI and Bcl-2 overexpression experiments. R.S.S., G.J.T. and D.C.L. provided the cortical-striatal brain-slice data. B.G.H. and B.R.S. wrote the manuscript.

## Competing financial interests

The authors declare no competing financial interests.

## Additional information

Supplementary information, chemical compound information and chemical probe information is available online at http://www.nature.com/naturechemicalbiology/. Reprints and permissions information is available online at http://npg.nature.com/reprintsandpermissions/. Correspondence and requests for materials should be addressed to B.R.S.